JOURNAL OF THERMOPHYSICS AND HEAT TRANSFER
Vol. 18, No. 2, April–June 2004

Thermal Contact Resistance of Nonconforming Rough Surfaces, Part 2: Thermal Model

M. Bahrami,* J. R. Culham,† M. M. Yovanovich,‡ and G. E. Schneider§
University of Waterloo, Waterloo, Ontario N2L 3G1, Canada

A new analytical model is developed for thermal contact resistance (TCR) of nonconforming rough surfaces. TCR is considered as the superposition of macro- and microthermal resistances. The effects of roughness, load, and radius of curvature on TCR are investigated. It is shown that there is a value of surface roughness that minimizes the TCR for a fixed load and geometry. Simple correlations for determining TCR, using relationships introduced in Part 1 of this study, are derived that cover the entire range of TCR from conforming rough to smooth spherical contacts. With introduction of an approximate model, it is shown that the effective microthermal resistance is not a function of surface curvature and contact pressure profile. The comparison of the present model with 600 experimental data points shows good agreement in the entire range of TCR. A criterion for conforming contacts is proposed that gives a range for the ratio of out-of-flatness to surface roughness.

Nomenclature

A	=	area, m^2
a	=	radius of contact, m
a'_L	=	relative radius of macrocontact, a_L/a_H
b	=	flux tube radius, m
b_L	=	specimen's radius, mm
B	=	relative macrocontact radius, a_L/b_L
c_1	=	Vickers microhardness coefficient, GPa
c_2	=	Vickers microhardness coefficient
d_v	=	Vickers indentation diagonal, μm
dr	=	increment in radial direction, m
E'	=	equivalent elastic modulus, GPa
F	=	external force, N
h	=	contact conductance, W/m^{2}K
H_{mic}	=	microhardness, GPa
H'	=	$c_1(1.62\sigma'/m)^{c_2}$, GPa
k	=	thermal conductivity, W/mK
m	=	mean absolute surface slope
n_s	=	number of microcontacts
P	=	pressure, Pa
P'_0	=	relative maximum pressure, $P_0/P_{0,H}$
Q	=	heat flow rate, W
R	=	thermal resistance, K/W
r, z	=	cylindrical coordinates
s	=	$0.95/(1+0.071c_2)$
Y	=	mean surface plane separation, m
α	=	nondimensional parameter, $\sigma\rho/a_H^2$
γ	=	general pressure distribution exponent
δ	=	maximum surface out-of-flatness, m
ε	=	flux tube relative radius, a_s/b_s
η_s	=	microcontacts density, m^{-2}
κ	=	H_B/H_{BGM}
λ	=	nondimensional separation, $Y/\sqrt{(2)}\sigma$
ξ	=	nondimensional radial position, r/a_L
ρ	=	radius of curvature, m
σ	=	rms surface roughness, μm
τ	=	nondimensional parameter, ρ/a_H
ψ	=	spreading resistance factor
Ω	=	nondimensional parameter

Subscripts

a	=	apparent
B	=	Brinell
b	=	bulk
c	=	critical
H	=	Hertz
j	=	joint
L	=	macro
mac	=	macro
mic	=	micro
p	=	plastic deformation
r	=	real
s	=	micro, solid
v	=	Vickers
0	=	value at origin
1, 2	=	solid 1, 2

Received 26 May 2003; presented as Paper 2003-4198 at the AIAA 36th Thermophysics Conference Meeting, Orlando, FL, 23 June 2003; revision received 11 August 2003; accepted for publication 13 August 2003.

*Ph.D. Candidate, Department of Mechanical Engineering; majid@mhtlab.uwaterloo.ca.
†Associate Professor, Director, Microelectronics Heat Transfer Laboratory.
‡Distinguished Professor Emeritus, Department of Mechanical Engineering. Fellow AIAA.
§Professor, Department of Mechanical Engineering. Associate Fellow AIAA.

Introduction

HEAT transfer across interfaces formed by mechanical contact of nonconforming rough solids occurs in a wide range of applications, such as microelectronics cooling, spacecraft structures, satellite bolted joints, nuclear engineering, ball bearings, and heat exchangers. Because of roughness of the contacting surfaces, real contacts in the form of microcontacts occur only at the top of surface asperities, which are a small portion of the nominal contact area, normally less than a few percent. As a result of curvature or out-of-flatness of the contacting bodies, a macrocontact area is formed, the area where the microcontacts are distributed.

Thermal energy can be transferred between contacting bodies by three different modes: 1) conduction, through the microcontacts, 2) conduction, through the interstitial fluid in the gap between the solids, and 3) thermal radiation across the gap if the interstitial substance is transparent to radiation. According to Clausing and Chao[1] radiation heat transfer across the interface remains small as long as the body temperatures are not too high, that is, less than 700 K, and in most typical applications can be neglected. In this study, the surrounding environment is a vacuum; thus, the only remaining heat

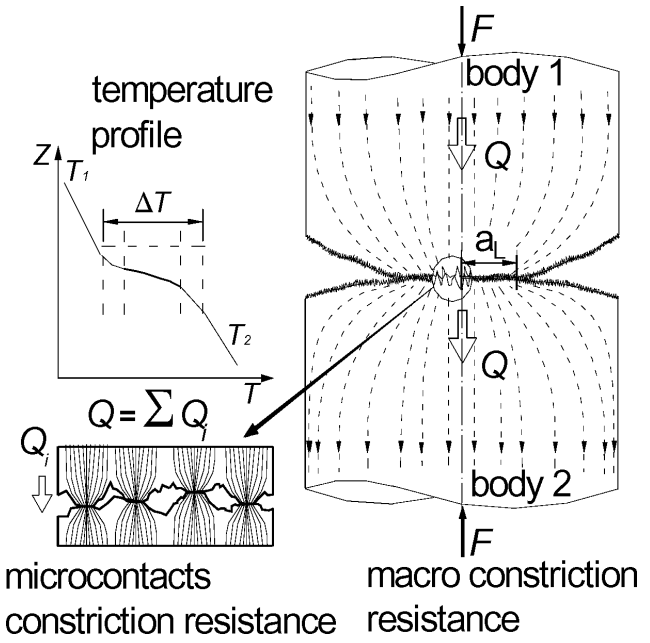

Fig. 1 Contact of two spherical rough surfaces in a vacuum.

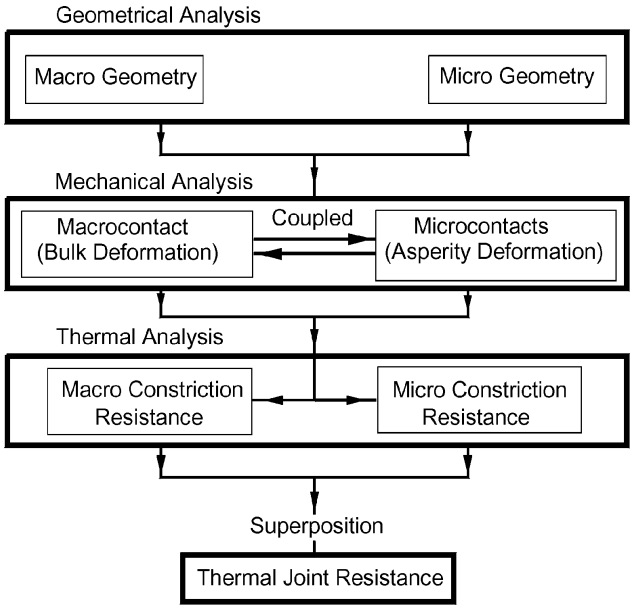

Fig. 2 Thermal contact problem.

transfer mode is conduction at the microcontacts. As illustrated in Fig. 1, heat flow is constrained to pass through the macrocontact and, then, in turn through the microcontacts. This phenomenon leads to a relatively high-temperature drop across the interface.

Two sets of resistances in series can be used to represent the thermal contact resistance (TCR) for a joint in a vacuum: the large-scale or macroscopic constriction resistance R_L and the small-scale or microscopic constriction resistance R_s (Refs. 1–3),

$$R_j = R_s + R_L \tag{1}$$

Many theoretical models for determining TCR have been developed for two limiting cases: 1) conforming rough, where contacting surfaces are assumed to be perfectly flat, and 2) elastoconstriction, where the effect of roughness is neglected, that is, contact of two smooth spherical surfaces. These two limiting cases are simplified cases of real contacts because engineering surfaces have both out-of-flatness and roughness simultaneously. As shown in Fig. 2, TCR problems basically consist of three separate problems: 1) geometrical, 2) mechanical, and 3) thermal; each subproblem also includes a micro- and macroscale component. The heart of TCR is the mechanical analysis. A mechanical model was developed and presented in Part 1 of this study.[4] The mechanical analysis determines the macrocontact radius and the effective pressure distribution for the large-scale contact problem, and the microcontact analysis gives the local separation between the mean planes of the contacting bodies, the local mean size and the number of microcontacts. The results of the mechanical analysis are used in the thermal analysis to calculate the microscopic and macroscopic thermal constriction resistances.

Few analytical models for contact of two nonconforming rough surfaces exist in the literature. Bahrami et al.[5] reviewed existing analytical nonconforming rough TCR models and showed through comparison with experimental data that none of the existing models cover the two mentioned limiting cases and the transition region in which both roughness and out-of-flatness are present and their effects on TCR are of the same importance.

Theoretical Background

Thermal spreading resistance is defined as the difference between the average temperature of the contact area and the average temperature of the heat sink/source, which is located far from the contact area, divided by the total heat flow rate Q (Ref. 6), $R = \Delta T/Q$. Thermal conductance is defined in the same manner as the film coefficient in convective heat transfer, $h = Q/(\Delta T A_a)$.

Considering the curvature or out-of-flatness of contacting surfaces in a comprehensive manner is very complex because of its random nature. Certain simplifications must be introduced to describe the macroscopic topography of surfaces using a few parameters. Theoretical approaches by Clausing and Chao,[1] Mikic and Rohsenow,[3] Yovanovich,[2] Nishino et al.,[7] and Lambert and Fletcher[8] assumed that a spherical profile might approximate the shape of the macroscopic nonuniformity. According to Lambert,[9] this assumption is justifiable because nominally flat engineering surfaces are often spherical, or crowned (convex) with a monotonic curvature in at least one direction. The approximate relationship between the radius of curvature and the maximum out-of-flatness, for relatively large radii of curvature (approaching flat), is[10]

$$\rho = b_L^2 \big/ 2\delta \tag{2}$$

where δ is the maximum out-of-flatness of the surface.

As discussed by Bahrami et al.,[4] the contact between two Gaussian rough surfaces can be approximated by the contact between a single Gaussian surface, having the effective surface characteristics, placed in contact with a perfectly smooth surface. The contact of two spheres can be replaced by a flat in contact with a sphere incorporating an effective radius of curvature,[11] effective surface roughness, and surface slope as given by

$$\sigma = \sqrt{\sigma_1^2 + \sigma_2^2}, \qquad m = \sqrt{m_1^2 + m_2^2}$$
$$1/\rho = 1/\rho_1 + 1/\rho_2 \tag{3}$$

Figure 3 summarizes the geometrical procedure, which has been widely used for modeling the actual contact between nonconforming rough bodies.

When two nonconforming random rough surfaces are placed in mechanical contact, many microcontacts are formed within the macrocontact area. Microcontacts are small and located far from each other. Thermal contact models are constructed based on the premise that inside the macrocontact area a number of parallel cylindrical heat channels exist. The real shapes of microcontacts can be a wide variety of singly connected areas depending on the local profile of the contacting asperities. Yovanovich et al.[12] studied the steady-state thermal constriction resistance of singly connected planar contacts of arbitrary shape. By using an integral formulation and a seminumerical integration process applicable to any shape, they proposed a definition for thermal constriction resistance based on the square root of the contact area. A nondimensional constriction resistance based on the square root of area was proposed,

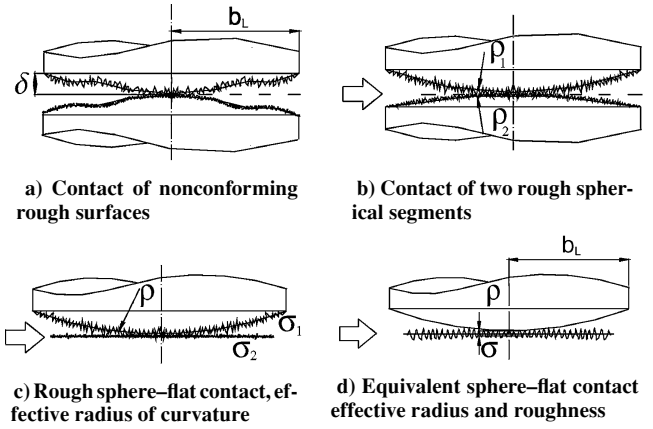

a) Contact of nonconforming rough surfaces

b) Contact of two rough spherical segments

c) Rough sphere–flat contact, effective radius of curvature

d) Equivalent sphere–flat contact effective radius and roughness

Fig. 3 Geometrical modeling.

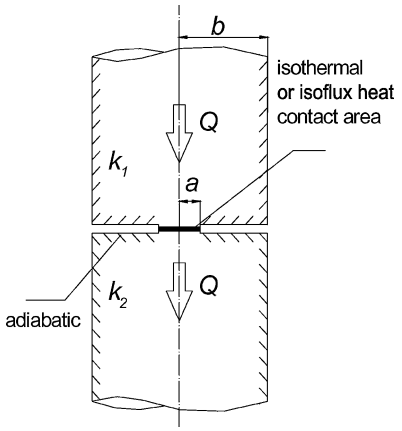

Fig. 4 Two flux tubes in series contact.

which varied by less than 5% for all shapes considered. Yovanovich et al.[12] concluded that the real shape of the contact was a second-order effect, and an equivalent circular contact, where surface area is preserved, can be used to represent the contact.

As the basic element for macro- and microthermal analysis, thermal constriction of the flux tube was employed by many researchers. Figure 4 shows two flux tubes in a series contact. A flux tube consists of a circular heat sink or source, which is in perfect thermal contact with a long tube. Heat enters the tube from the source and leaves the tube at the other end. Cooper et al.[13] proposed a simple, accurate correlation for calculating the thermal spreading resistance of the isothermal flux tube,

$$R_{\text{flux tube 1}} + R_{\text{flux tube 2}} = \psi(\varepsilon)/2k_s a = (1-\varepsilon)^{1.5}\big/2k_s a \qquad (4)$$

where $\varepsilon = a/b$, $k_s = 2k_1k_2/(k_1+k_2)$, and $\psi(\cdot)$ is the spreading resistance factor. (See Bahrami et al.[5] for more detail.) In Eq. (4), it is assumed that the radii of two contacting bodies are the same, that is, $b_1 = b_2 = b$. For the general case where $b_1 \neq b_2$, thermal spreading resistance will be $R_{\text{flux tube}} = \psi(a/b)/4ka$.

Figure 5 shows the thermal resistance network for nonconforming rough contacts. The total or joint resistance can be written as

$$R_j = R_{L,1} + R_{s,1} + R_{s,2} + R_{L,2} \qquad (5)$$

where

$$\left(\frac{1}{R_s}\right)_{1,2} = \left(\sum_{i=1}^{n_s}\frac{1}{R_{s,i}}\right)_{1,2} \qquad (6)$$

where n_s and $R_{s,i}$ are the number of microcontacts and the resistance of each microcontact, respectively. Subscripts 1 and 2 signify bodies 1 and 2.

Present Model

In addition to the geometrical and mechanical assumptions, which were discussed in Part 1 of this study,[4] the remaining assumptions of the present model are as follows:

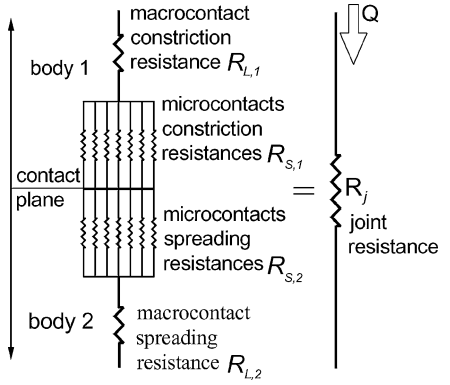

Fig. 5 Thermal resistance network for nonconforming rough contacts in a vacuum.

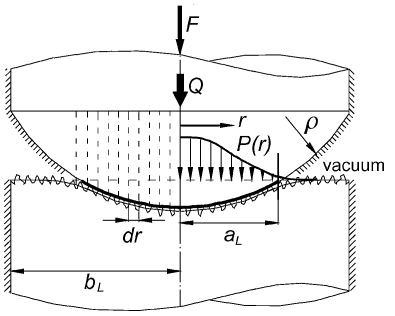

Fig. 6 Geometry of contact.

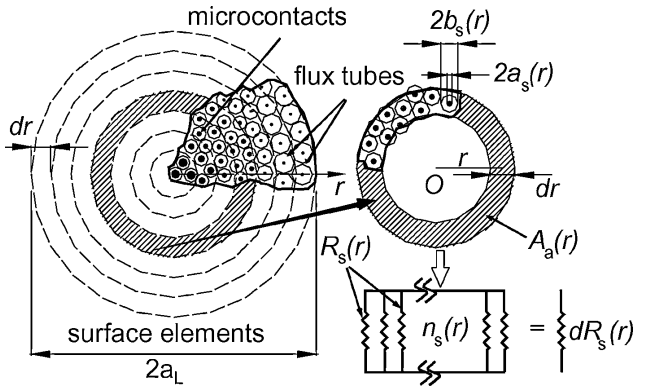

Fig. 7 Microcontacts distribution in contact area and thermal resistance network for a surface element.

1) Contacting solids are isotropic and thick relative to the roughness.

2) Radiation heat transfer is negligible.

3) Microcontacts are circular, and there is steady-state heat transfer at microcontacts.

4) Microcontacts are isothermal. Cooper et al.[13] proved that all microcontacts must be at the same temperature provided the conductivity in each body is independent of direction, position, and temperature.

5) Surfaces are clean, and the contact is static.

Figure 6 shows the geometry of the contact with equivalent radius of curvature and roughness, where a_L is the radius of the macrocontact area and b_L is the radius of the contacting bodies.

The flux tube solution is employed to determine the macrocontact thermal resistance, that is,

$$R_L = \frac{(1-a_L/b_L)^{1.5}}{2k_s a_L} \qquad (7)$$

Separation between the mean planes of contacting bodies and pressure distribution are not uniform in the contact area; consequently, the number and the average size of microcontacts decrease as the radial position r increases. Figure 7 shows the modeled geometry of the microcontact distribution (macrocontact area the circle with radius a_L) is divided into surface elements, where dashed rings

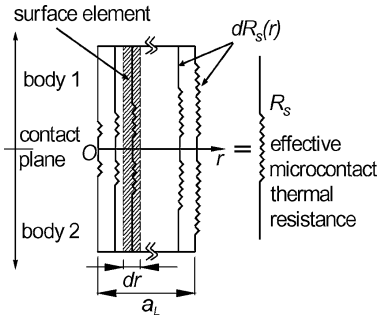

Fig. 8 Thermal resistance network for surface elements.

have increment dr. Figure 7 shows the mean average size of microcontacts as small filled circles. Around each microcontact, a dashed circle illustrates the flux tube associated with the microcontact. Whereas microcontacts can vary in both size and shape, a circular contact of equivalent area can be used to approximate the actual microcontacts because the local separation is uniform in each surface element.

Local spreading resistance for microcontacts can be calculated by applying the flux tube expression

$$R_s(r) = \frac{\psi[\varepsilon(r)]}{2k_s a_s(r)} \tag{8}$$

where $\varepsilon(r) = a_s(r)/b_s(r)$ is the local microcontacts relative radius and $a_s(r)$ and $\psi(\cdot)$ are the local mean average microcontact radius and the spreading resistance factor given by Eq. (4).

The microcontacts local density and relative radius can be calculated from[4]

$$\varepsilon(r) = \sqrt{A_r(r)/A_a(r)} = \sqrt{\tfrac{1}{2}\text{erfc }\lambda(r)} \tag{9}$$

$$n_s(r) = \tfrac{1}{16}(m/\sigma)^2\{\exp[-2\lambda^2(r)]/\text{erfc }\lambda(r)\}A_a \tag{10}$$

where $\lambda(r) = Y(r)/\sqrt{(2)}\sigma$, A_r, and A_a are nondimensional separation and the real and the apparent contact area, respectively.

The thermal resistance network for a surface element dr is shown in Fig. 7. In each element $n_s(r)$ microcontacts exist that provide identical parallel paths for transferring thermal energy. Therefore, microcontact thermal resistance for a surface element $dR_s(r)$ is

$$dR_s(r) = R_s(r)/n_s(r) \tag{11}$$

As shown in Fig. 8, surface elements form another set of parallel paths for transferring thermal energy in the macrocontact area. Therefore, the effective microthermal resistance for the joint is

$$R_s = 1\Big/\sum 1/dR_s(r) \tag{12}$$

The joint resistance is the sum of the macro- and microthermal resistances, that is, Eq. (1).

Results

As explained in Part 1,[4] a simulation routine was developed to calculate the thermal joint resistance. As an example, contact of a 25-mm sphere with a flat was considered and solved with the routine. The contacting bodies are stainless steel and have a 1.41-μm equivalent roughness. Table 1 lists the contact parameters. The mechanical results were presented in Part 1,[4] and Figs. 9 and 10 present thermal outputs. As expected, the thermal resistance of the microcontacts (resistance of the local mean microcontact) increases as r increases. The microcontact relative radius ε has its maximum value at the center of the contact and decreases with increasing radial position r.

To investigate the effect of input parameters on thermal joint resistance R_j and its components, that is, the macro R_L and the micro R_s thermal resistances, the simulation routine was run for a range of each input parameter, while the remaining parameters in Table 1 were held constant. Additionally, elastoconstriction thermal resistance introduced by Yovanovich,[14] indicated by R_H, was also included in the study. Elastoconstriction is a limiting case in which the surfaces are assumed to be perfectly smooth, that is, $a_L = a_H$ and $R_s = 0$.

Table 1 Input parameters for a typical contact problem

Parameters	Value
ρ	25 mm
σ	1.41 μm
m	0.107
b_L	25 mm
F	50 N
E'	112.1 GPa
c_1/c_2	6.27 GPa/−0.15
k_s	16 W/mK

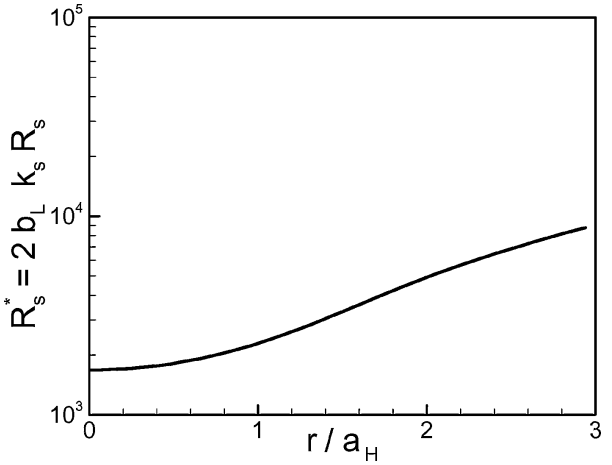

Fig. 9 Microthermal contact resistance.

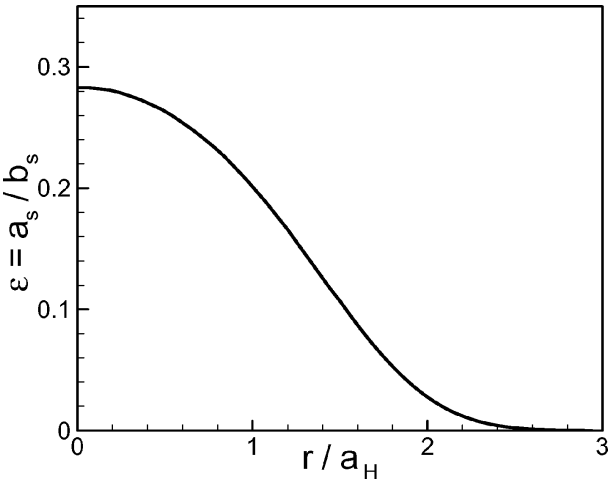

Fig. 10 Microcontact relative radius.

The effect of roughness on macro-, micro-, and joint resistances are shown in Fig. 11. Recall that the joint resistance is the summation of the macro- and microcontact resistances. With relatively small roughness, the macrothermal resistance dominates the joint resistance and the microthermal resistance is negligible; also the joint resistance is close to the elastoconstriction thermal resistance. By increasing roughness, a_L becomes larger; thus, the macrothermal resistance decreases and the microthermal resistance increases, and at some point they become comparable in size. An additional increase in the surface roughness leads to a situation where the microthermal resistance controls the joint resistance. It also can be seen from Fig. 11 that for a fixed geometry and load, there is a roughness that minimizes the thermal joint resistance.

The effect of load on micro-, macro-, and joint thermal resistances is shown in Fig. 12. At light loads, because of the small number and size of the microcontacts, the microthermal resistance dominates. As the load increases, the joint resistance decreases continuously, micro- and macrothermal resistances become comparable in size,

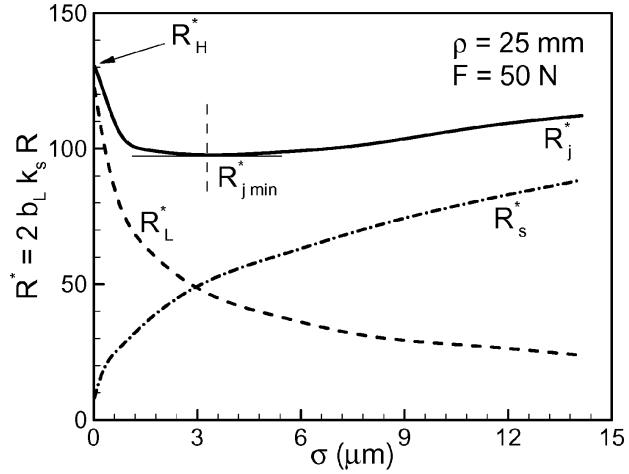

Fig. 11 Effect of roughness on TCR.

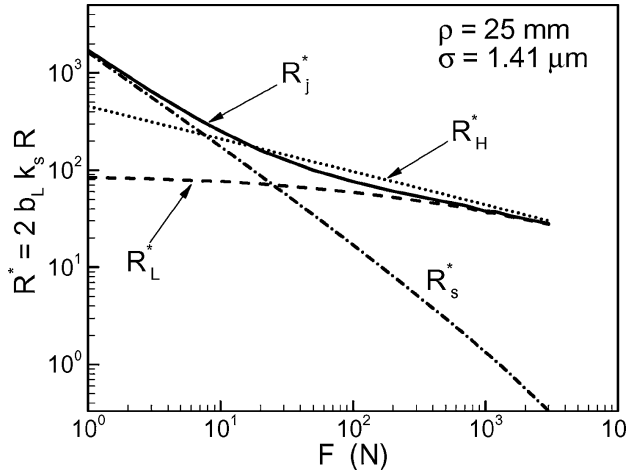

Fig. 12 Effect of load on TCR.

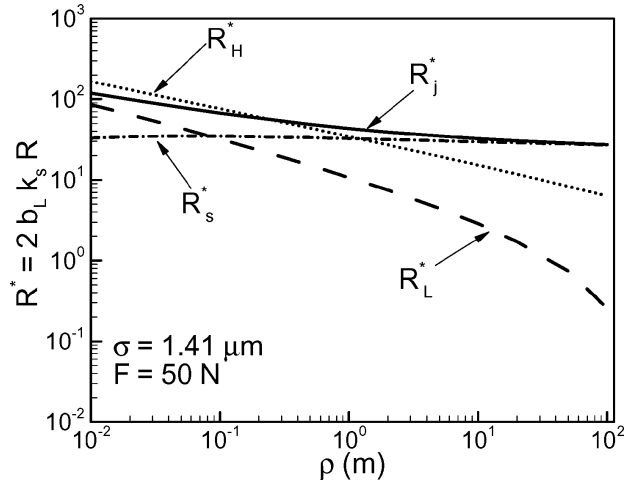

Fig. 13 Effect of radius of curvature on TCR.

and, at larger loads, the macrothermal resistance becomes the controlling part. At higher loads, the joint resistance approaches the elastoconstriction resistance as if no roughness exists.

Figure 13 shows the effect of radius of curvature. At very small radii, the macrothermal resistance dominates due to the small size of macrocontacts. As the radius of curvature increases, approaching the flat surface, the microthermal resistance becomes more important, and the macro resistance becomes smaller. Eventually when $a_L = b_L$, the macroresistance falls to zero. Note that the microthermal resistance does not change as the surface curvature ρ varies over a wide range. This is a very important trend and will be discussed later.

Alternative Approach

The goal of this study is to develop simple correlations for determining TCR. In this section, a general expression for the microthermal spreading resistance is derived, which, in conjunction with the macrothermal resistance, Eq. (7), gives a correlation to calculate the thermal joint resistance in a vacuum environment.

The amount of heat transferred in a nonconforming rough contact is

$$Q = \sum \mathrm{d}Q = \iint_{\text{contact plane}} \mathrm{d}Q \tag{13}$$

where $\mathrm{d}Q$ is the heat transferred in a surface element. The local thermal joint conductance is a function of r

$$Q = \iint_{\text{contact plane}} h_s(r)\Delta T_s \,\mathrm{d}A_a \tag{14}$$

where $\mathrm{d}A_a$ and $\Delta T_s =$ constant are the area of a surface element and the temperature drop, respectively. Because the macrocontact area is approximated as a circle,

$$Q = 2\pi\,\Delta T_s \int_0^{a_L} h_s(r) r \,\mathrm{d}r \tag{15}$$

The effective thermal microconductance for a joint can be defined as $h_s = Q/A_a\Delta T_s$. Therefore, the effective microcontact conductance can be found from

$$h_s = \frac{2\pi}{A_a}\int_0^{a_L} h_s(r) r \,\mathrm{d}r \tag{16}$$

or in terms of thermal resistance, where $R = 1/(hA_a)$,

$$R_s = \frac{1}{2\pi}\left[\int_0^{a_L} h_s(r) r \,\mathrm{d}r\right]^{-1} \tag{17}$$

Yovanovich[15] proposed an accurate expression for determining the thermal conductance of conforming rough contacts,

$$h_s = 1.25 k_s (m/\sigma)(P/H_{\text{mic}})^{0.95} \tag{18}$$

where H_{mic} is the microhardness of the softer material in contact. When Eqs. (17) and (18) are combined, a relationship between thermal microresistance and pressure distribution can be found,

$$R_s = \frac{\sigma}{2.5\pi m k_s}\left\{\int_0^{a_L}\left[\frac{P(r)}{H_{\text{mic}}(r)}\right]^{0.95} r \,\mathrm{d}r\right\}^{-1} \tag{19}$$

Microhardness depends on several parameters: mean surface roughness σ, mean absolute slope of asperities m, type of material, method of surface preparation, and applied pressure. According to Hegazy,[16] surface microhardness can be introduced into the calculation of relative contact pressure in the form of the Vickers microhardness,

$$H_v = c_1 (d_v')^{c_2} \tag{20}$$

where H_v is the Vickers microhardness in gigapascal, $d_v' = d_v/d_0$, where $d_0 = 1\ \mu$m, and c_1 and c_2 are correlation coefficients determined from Vickers microhardness measurements. Song and Yovanovich[17] developed an explicit expression relating microhardness to the applied pressure

$$P/H_{\text{mic}} = (P/H')^{1/1+0.071c_2} \tag{21}$$

where $H' = c_1(1.62\sigma'/m)^{c_2}$, $\sigma' = \sigma/\sigma_0$, and $\sigma_0 = 1\ \mu$m.

Sridhar and Yovanovich[18] developed empirical relations to estimate the Vickers microhardness coefficients, using the bulk hardness of the material. Two least-square-cubic fit expressions were reported:

$$c_1 = H_{BGM}(4.0 - 5.77\kappa + 4.0\kappa^2 - 0.61\kappa^3) \tag{22}$$

$$c_2 = -0.57 + (1/1.22)\kappa - (1/2.42)\kappa^2 + (1/16.58)\kappa^3 \tag{23}$$

where $\kappa = H_B/H_{BGM}$, H_B is the Brinell hardness of the bulk material, and $H_{BGM} = 3.178$ GPa. The preceding correlations are valid for the range $1.3 \le H_B \le 7.6$ GPa with the rms percent difference between data and calculated values reported to be 5.3 and 20.8% for c_1 and c_2, respectively. However, in situations where an effective value for microhardness $H_{\text{mic},e}$ is known, the microhardness coefficients can be calculated from $c_1 = H_{\text{mic},e}$ and $c_2 = 0$.

Combining Eqs. (19) and (21) gives

$$R_s = \frac{\sigma H'^s}{2.5\pi k_s m}\left\{\int_0^{a_L} [P(r)]^s r\, \mathrm{d}r\right\}^{-1} \tag{24}$$

where $s = 0.95/(1 + 0.071c_2)$. A general pressure distribution was proposed in Part 1 of this study,[4] which covers the entire spherical rough contacts including flat contacts,

$$P(\xi) = \begin{cases} F/\pi b_L^2 & F_c = 0 \\ P_0(1-\xi^2)^\gamma & F \le F_c \\ P_{0,c}(1-\xi^2)^{\gamma_c} + (F - F_c)/\pi b_L^2 & F \ge F_c \end{cases} \tag{25}$$

where $\xi = r/a_L$ and $\gamma = 1.5(P_0/P_{0,H})(a_L/a_H)^2 - 1$. F_c is the critical force where $a_L = b_L$, and it is given by

$$F_c = (4E'/3\rho)\left[\max\left\{0, \left(b_L^2 - 2.25\sigma\rho\right)\right\}\right]^{\frac{3}{2}} \tag{26}$$

where max $\{x, y\}$ returns the maximum value between x and y. Substituting the pressure distribution for $F \le F_c$ into Eq. (24), we obtain

$$R_s = \frac{\sigma (H'/P_0)^s}{2.5\pi m k_s a_L^2}\left[\int_0^1 (1-\xi^2)^{s\gamma}\xi\, \mathrm{d}\xi\right]^{-1} \tag{27}$$

After evaluating and simplifying the integral, we obtain

$$R_s = \frac{\sigma(1+s\gamma)}{1.25\pi m k_s a_L^2}\left(\frac{H'}{P_0}\right)^s \tag{28}$$

For $F \ge F_c$, the effective microcontact thermal resistance, following the same method, becomes

$$R_s = \frac{\sigma}{1.25\pi m k_s b_L^2}\left[\left(\frac{H'}{P_{0,c}}\right)^s (1+s\gamma_c) + \left(\frac{\pi H' b_L^2}{F - F_c}\right)^s\right] \tag{29}$$

where $P_{0,c}$ and γ_c are the values at the critical force. The general relationship for microthermal resistance can be summarized as

$$R_s^* = \begin{cases} \left(\pi H' b_L^2/F\right)^s & F_c = 0 \\ (b_L/a_L)^2 (H'/P_0)^s (1+s\gamma) & F \le F_c \\ (H'/P_{0,c})^s (1+s\gamma_c) + \left[\pi H' b_L^2/(F - F_c)\right]^s & F \ge F_c \end{cases} \tag{30}$$

where $R_s^* = 1.25\pi b_L^2 k_s (m/\sigma) R_s$.

Equation (30) can be simplified by introducing an approximation. Because the Vickers coefficient c_2 is negative and in the range of $-0.35 \le c_2 \le 0$, the parameter $s = 0.95/(1 + 0.071c_2)$ is close to one, that is, $0.95 \le s \le 0.97$ and can be approximated as $s = 1$. When this simplification, is introduced, the microthermal resistance R_s, that is, Eq. (24) simplifies to

$$R_s = \frac{\sigma H'}{2.5\pi k_s m}\left[\int_0^{a_L} P(r) r\, \mathrm{d}r\right]^{-1} \tag{31}$$

From a force balance, one can write

$$F = 2\pi \int_0^{a_L} P(r) r\, \mathrm{d}r$$

and Eq. (31) becomes

$$R_s = (H'/1.57 k_s F)(\sigma/m) \tag{32}$$

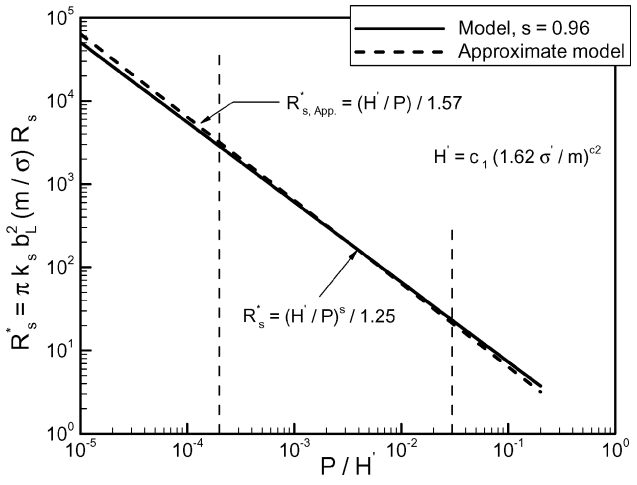

Fig. 14 Comparison between approximate and full model, conforming rough contacts.

where the leading constant in Eq. (18) has been changed from 1.25 to 1.57 to compensate for introducing the approximation, where the exponent s is set one. The approximate model, Eq. (32), is compared with the full model for conforming rough contacts, [the first of Eqs. (30)] in Fig. 14, where an average value of $s = 0.96$ was chosen. It can be seen that the approximate model shows good agreement with the full model in the range of $2 \times 10^{-4} \le P/H' \le 5 \times 10^{-2}$, which includes a wide range of loading, that is, moderate and high loads. The difference between the approximate and the full model increases in light loads, $P/H' < 10^{-4}$.

Equation (32) is general and applicable to all contact geometries, that is, conforming and non-conforming rough contacts. With use of the approximate model, the microthermal resistance R_s becomes simpler to apply. In addition, the approximate effective microthermal resistance is independent of the surface curvature. This trend can also be observed in Fig. 13, where it should be noted that the full model (computer program) with no simplifications was used to construct the plot. Also from the approximate relationship, it can be concluded that the profile of the pressure distribution does not effect the effective microthermal resistance.

Superimposing Eqs. (7) and (32), the joint resistance, using the approximate R_s, is found:

$$R_j = \frac{H'}{1.57 k_s F}\left(\frac{\sigma}{m}\right) + \frac{(1 - a_L/b_L)^{1.5}}{2k_s a_L} \tag{33}$$

From Eq. (33) one can conclude that 1) the effective microthermal resistance, except for the thermal conductivity, is only a function of the contact microscale characteristics, that is, surface roughness σ, slope m, microhardness H', and load F, and 2) on the other hand, the macrothermal resistance is a function of the macroscale contact parameters, the macrocontact radius a_L, and size of the contacting bodies b_L. These conclusions are in agreement with the TCR analysis in Fig. 2. From Part 1 of this study,[4] we know that the macrocontact radius is a function of the effective elasticity modulus E', radius of curvature ρ, surface roughness σ, and the load F.

The applied load and the surface roughness appear to play important roles in both macro- and microthermal resistances. The effect of surface roughness on the macroresistance is limited to the macrocontact radius a_L. The applied load is the connecting bridge between the macro- and micromechanical analyses because the force balance must be satisfied in both analyses.

Comparison with Experimental Data

During the last four decades, a large number of experimental data have been collected for a wide variety of materials such as brass, magnesium, nickel 200, silver, and stainless steel (SS) in a vacuum. About 600 data points were collected from an extensive review of the literature and summarized and compared with the present model. As summarized in Table 2, the experimental data form a complete

set of the materials with a wide range of mechanical, thermal, and surfaces characteristics used in applications where TCR is of concern. The data also include the contact between dissimilar metals such as Ni200–Ag and SS–carbon steel (CS).

Generally, TCR experimental procedures include two cylindrical specimens of the same diameter b_L, which are pressed coaxially together by applying an external load in a vacuum chamber. After reaching steady-state conditions, TCR is measured at each load. These experiments have been conducted by many researchers such as Burde[19] and Clausing and Chao.[1] Table 3 indicates the researchers, reference publications, specimen designation, and the material type used in the experiments (Refs. 1, 3, 16, and 19–24).

Table 2 Range of parameters for the experimental data

Parameter	Range
b_L, mm	7.15–14.28
P/H'	5.4×10^{-6}–0.02
E', GPa	25.64–114.0
F, N	7.72–16,763.9
k_s, W/mK	16.6–227.2
m	0.04–0.34
σ, μm	0.12–13.94
ρ, m	0.013–120

Table 3 Reseacher and specimen materials used in comparisons

Ref.	Researcher	Material
A	Antonetti[23]	Ni200
		Ni200–Ag
B	Burde[19]	SPS 245, CS
CC	Clausing–Chao[1]	Al2024 T4
		Brass Anaconda
		Mg AZ 31B
		SS303
F	Fisher[20]	Ni 200–CS
H	Hegazy[16]	Ni200
		SS304
		Zircaloy4
		Zr-2.5%wt Nb
K	Kitscha[21]	Steel 1020–CS
MM	McMillan–Mikic[24]	SS303
MR	Mikic–Rohsenow[3]	SS305
M	Milanez et al.[22]	SS304

The comparison includes all three regions of TCR, that is, the conforming rough, the elastoconstriction, and the transition. Tables 4 and 5 list the experiment number, that is, the number that was originally assigned to a particular experimental data set by the researchers, and geometrical, mechanical, and thermal properties of the experimental data, as reported. Clausing and Chao,[1] Fisher,[20] Kitscha,[21] and Mikic and Rohsenow[3] did not report the surface slope m; the Lambert and Fletcher[8] correlation was used to estimate these values (see Part 1[4]). Additionally, the exact values of radii of curvature for conforming rough surfaces were not reported. Because these surfaces were prepared to be optically flat, radii of curvature in the order of $\rho \approx 100$ m are considered for these surfaces.

Figure 15 shows the comparison between the present model and the experimental data, with Eqs. (7) and (20), where

$$R_j^* = k_s b_L R_j$$

$$\Omega = \frac{(1-B)^{1.5}}{2B} + \begin{cases} \dfrac{(\sigma/m)}{1.25\pi b_L}\left(\dfrac{H'}{P}\right)^s & F_c = 0 \\ \dfrac{(\sigma/m)(1+s\gamma)}{1.25\pi b_L B^2}\left(\dfrac{H'}{P_0}\right)^s & F \le F_c \\ \dfrac{(\sigma/m)}{1.25\pi b_L}\left\{\left(\dfrac{H'}{P_{0,c}}\right)^s (1+s\gamma_c) + \left(\dfrac{\pi H' b_L^2}{(F-F_c)}\right)^s\right\} & F \ge F_c \end{cases} \tag{34}$$

where $B = a_L/b_L \le 1$ and $P_0 = P_{0,H}/(1+1.37\alpha\tau^{-0.075})$ is the maximum contact pressure. The parameter Ω is the nondimensional TCR predicted by the (full) model, that is, $\Omega = R_s^* + R_j^*$ or $R_j^* = \Omega$. Therefore, the model is shown by a 45-deg line in Fig. 15. The macrocontact radius a_L can be determined from[4]

$$a_L = a_H\left(1.80\sqrt{\alpha + 0.31\tau^{0.056}}\Big/\tau^{0.028}\right) \tag{35}$$

Using Eq. (35), a relationship for B can be found as a function of nondimensional and geometrical parameters,

$$B = a_L/b_L = \max\left\{1,\ 1.80(a_H/b_L)\left(\sqrt{\alpha + 0.31\tau^{0.056}}\Big/\tau^{0.028}\right)\right\} \tag{36}$$

Table 4 Geometrical, mechanical, and thermophysical properties, rough sphere–flat contacts

Ref.	E', GPa	σ, μm/m	ρ, m	c_1, GPa/c_2	k_s, W/mk	b_L, mm
B,A-1	114.0	0.63/0.04	0.013	3.9/0	40.7	7.2
B,A-2	114.0	1.31/0.07	0.014	3.9/0	40.7	7.2
B,A-3	114.0	2.44/0.22	0.014	3.9/0	40.7	7.2
B,A-4	114.0	2.56/0.08	0.019	4.4/0	40.7	7.2
B,A-5	114.0	2.59/0.10	0.025	4.4/0	40.7	7.2
B,A-6	114.0	2.58/0.10	0.038	4.4/0	40.7	7.2
CC,1A	38.66	0.42/-	14.0	1.6/−0.04	141	12.7
CC,8A	38.66	2.26/-	14.7	1.6/−0.04	141	12.7
CC,1B	49.62	0.47/-	3.87	3.0/−0.17	125	12.7
CC,2B	49.62	0.51/-	4.07	3.0/−0.17	125	12.7
CC,3B	49.62	0.51/-	3.34	3.0/−0.17	102	12.7
CC,4B	49.62	0.51/-	4.07	3.0/−0.17	125	12.7
CC,3S	113.7	0.11/-	21.2	4.6/−0.13	17.8	12.7
F,11A	113.1	0.12/-	0.019	4.0/0	57.9	12.5
F,11B	113.1	0.12/-	0.038	4.0/0	57.9	12.5
F,13A	113.1	0.06/-	0.038	4.0/0	58.1	12.5
K,T1	113.8	0.76/-	0.014	4.0/0	51.4	12.7
K,T2	113.8	0.13/-	0.014	4.0/0	51.4	12.7
MM,T1	113.7	2.7/0.06	0.128	4.0/0	17.3	12.7
MM,T2	113.7	1.75/0.07	2.44	4.0/0	22	12.7
MR,T1	107.1	4.83/-	21.2	4.2/0	19.9	12.7
MR,T2	107.1	3.87/-	39.7	4.2/0	19.9	12.7

Table 5 Geometrical, mechanical, and thermophysical properties for conforming rough contacts

Ref.	E', GPa	σ, μm	m	c_1, GPa	c_2	k_s, W/mk	b_L, mm
A,P3435	112.1	8.48	0.34	6.3	−0.26	67.1	14.3
A,P2627	112.1	1.23	0.14	6.3	−0.26	64.5	14.3
A,P1011	112.1	4.27	0.24	6.3	−0.26	67.7	14.3
A,P0809	112.1	4.29	0.24	6.3	−0.26	67.2	14.3
A,P1617	63.9	4.46	0.25	0.39	0	100	14.3
A,P3233	63.9	8.03	0.35	0.39	0	100	14.3
H,NI12	112.1	3.43	0.11	6.3	−0.26	75.3	12.5
H,NI34	112.1	4.24	0.19	6.3	−0.26	76.0	12.5
H,NI56	112.1	9.53	0.19	6.3	−0.26	75.9	12.5
H,NI78	112.1	13.9	0.23	6.3	−0.26	75.7	12.5
H,NI910	112.1	0.48	0.23	6.3	−0.26	75.8	12.5
H,SS12	112.1	2.71	0.07	6.3	−0.23	19.2	12.5
H,SS34	112.1	5.88	0.12	6.3	−0.23	19.1	12.5
H,SS56	112.1	10.9	0.15	6.3	−0.23	18.9	12.5
H,SS78	112.1	0.61	0.19	6.3	−0.23	18.9	12.5
H,Z412	57.3	2.75	0.05	3.3	−0.15	16.6	12.5
H,Z434	57.3	3.14	0.15	3.3	−0.15	17.5	12.5
H,Z456	57.3	7.92	0.13	3.3	−0.15	18.6	12.5
H,Z478	57.3	0.92	0.21	3.3	−0.15	18.6	12.5
H,ZN12	57.3	2.50	0.08	5.9	−0.27	21.3	12.5
H,ZN34	57.3	5.99	0.16	5.9	−0.27	21.2	12.5
H,ZN56	57.3	5.99	0.18	5.9	−0.27	21.2	12.5
H,ZN78	57.3	8.81	0.20	5.9	−0.27	21.2	12.5
M,SS1	113.8	0.72	0.04	6.3	−0.23	18.8	12.5

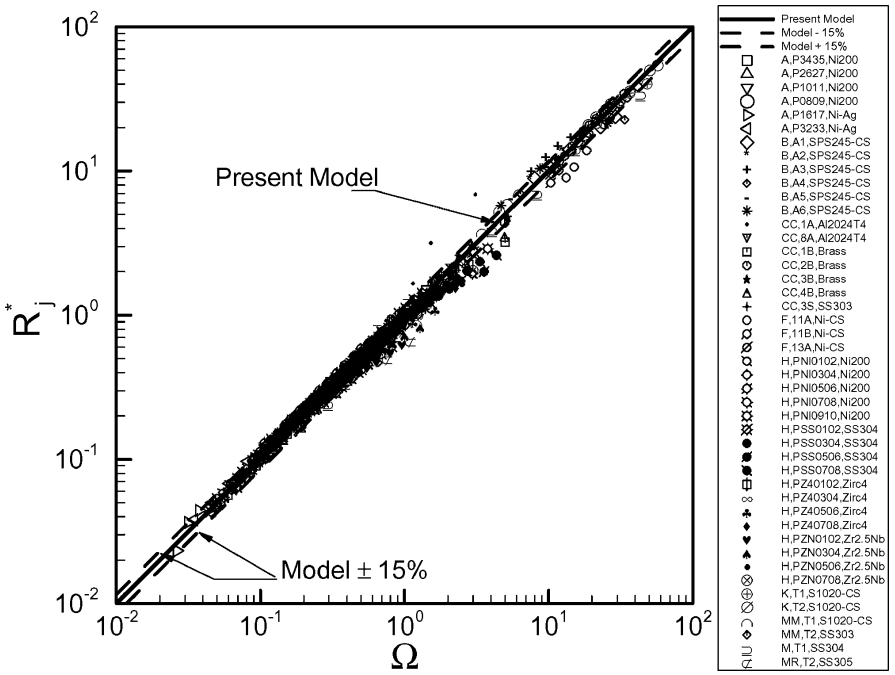

Fig. 15 Comparison of present model with experimental data.

Experimental data are distributed over four decades of Ω from approximately 0.03 up to 70. The model shows good agreement with data over the entire range of comparison with the exception of a few points. The approximate model [Eq. (33)] was also compared with experimental data using the same method and showed good agreement; because the plots are almost identical, a direct comparison of the approximate model with data is not presented.

In most of the conforming rough data sets, such as that of Hegazy,[16] experimental data show a lower resistance at relatively light loads in comparison with the model, and the data approach the model as the load increases. This trend can be observed in almost all conforming rough data sets (Fig. 15). This phenomenon, which is called the truncation effect,[22] is important at light loads when surfaces are relatively rough. A possible reason for this behavior is the Gaussian assumption of the surface asperities, which implies that asperities with infinite heights exist. Milanez et al.[22] experimentally studied the truncation effect and proposed correlations for maximum asperities heights as functions of surface roughness.

If the external load increases beyond the elastic limit of the contacting bodies, elastoplastic and plastic deformations occur. The plastic macrocontact radius a_P is larger than the elastic radius a_L, that is $a_P > a_L$. Consequently, lower TCR will be measured; this trend can be clearly seen in the Fisher[20] data sets F,11A,Ni–CS (Fig. 15).

The accuracy of experimental data were reported by Antonetti,[23] Fisher,[20] and Hegazy[16] to be 8.1, 5, and 7%, respectively. Unfortunately, the uncertainty of other researchers' data is not available. Because of the mentioned approximations to account for unreported data, the accuracy of the full model is difficult to assess. However,

the rms and the average absolute difference between the model and data are approximately 13.6 and 9.3%, respectively. The rms and the average absolute difference between the approximate model and data are approximately 14.8 and 10.9%, respectively, as a result of choosing the constant in Eq. (32) to be 1.57.

Criterion for Conforming Contacts

A criterion for determining a flat surface was derived in Part 1 of this study,[4] implying that when the effect of surface curvature on contact pressure distribution is negligible the surface is ideally flat. It was shown that if the surface roughness and curvature are in the same order of magnitude, that is, $\delta/\sigma \sim 1$ with no load applied, the macrocontact reaches the edge of the contacting bodies and $a_L = b_L$.

From the TCR point of view, the conforming or flat contact can be defined as a contact in which the macrothermal resistance R_L is negligible. As already discussed, surface curvature has no effect on the microthermal resistance (the approximate model). Thus, the effect of surface curvature is limited to the macrothermal resistance R_L.

The macrothermal resistance is determined from Eq. (7), which can be rewritten in the nondimensional form as

$$R_L^* = k_s R_L b_L = (1 - B)^{1.5}/2B \tag{37}$$

where $B = a_L/b_L \leq 1$. As shown in Fig. 16, the macrothermal resistance is zero at $B = 1$, that is, $a_L = b_L$ (perfectly flat contacts); as B decreases from 1 to 0.8, the macrothermal resistance increases from 0 to 0.05. This increase is relatively small and considered negligible. Therefore, it is reasonable to set the flat contact criterion to $B = 0.8$, where the macro thermal resistance is almost negligible. Note that for $0.8 \leq B \leq 1$ (large radii of curvature) the microthermal resistance controls the joint resistance (Fig. 13).

A correlation for determining the macrocontact radius a_L was proposed in Part 1 of this study[4] for surfaces with relatively large radii of curvature, $a_L = 1.5 a_H \sqrt{(\alpha + 0.45)}$. Using this relationship, one can write $B = 0.8 = 1.5(a_H/b_L)\sqrt{(\alpha + 0.45)}$. Substituting the nondimensional parameter, $\alpha = \sigma\rho/a_H^2$ and Eq. (2), we obtain

$$\sigma/\delta = 2\left[0.28 - 0.45(a_H/b_L)^2\right] \tag{38}$$

As can be seen from Eq. (38), the relative out-of-flatness is a function of a_H/b_L, which contains the applied load, the elastic properties, and the geometry of the contacting bodies. As shown in Part 1,[4] an increase in surface roughness results in an increase in the macrocontact radius. When $B = a_L/b_L = 0.8$ is set, depending on the level of surface roughness, a range for a_H/b_L can be estimated, approximately $0.7 \leq a_L/a_H \leq 0.96$, which results in $0.56 \leq a_H/b_L \leq 0.77$. This range means that the increase in the macrocontact radius (compared to the smooth Hertzian radius) is within a 5–30% increase. It is a reasonable estimate, when it is noted that we are investigating the contact of surfaces with relatively large radii of curvature under light loads. When Eq. (38) and the mentioned range for a_H/b_L are combined, a range for δ/σ can be found for flat contacts, approximately $3 \leq \delta/\sigma \leq 30$ from very rough to very smooth surfaces, respectively.

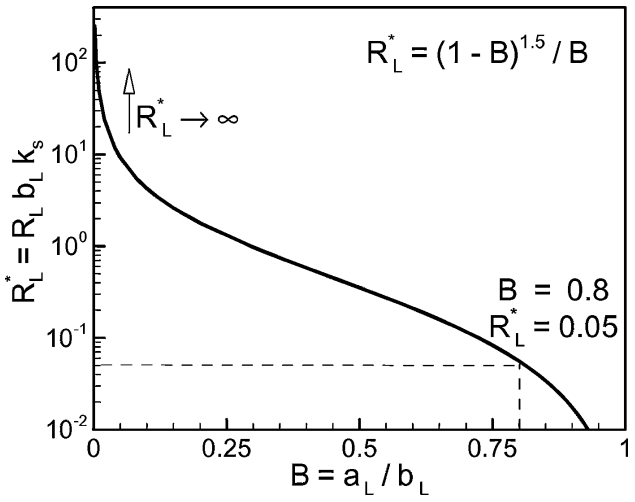

Fig. 16 Macrothermal resistance.

Conclusions

TCR of nonconforming rough surfaces was considered as the superposition of macro- and microthermal resistance components accounting for the effects of surface curvature and roughness, respectively. TCR problems were categorized into three main regions: 1) the conforming rough limit, where the contacting surfaces are flat and the effect of surface curvature can be ignored, and thus, the microthermal resistance dominates the joint resistance; 2) the elastoconstriction limit, in which the radii of the contacting bodies are relatively small and the effect of roughness on the TCR is negligible and the macro resistance is the controlling part; and 3) the transition region, where the macro- and microthermal resistances are comparable.

The results of the mechanical model presented by Bahrami et al.,[4] that is, the local mean separation, the local mean radius, and the number of microcontacts, were used to develop an analytical thermal model for determining TCR of nonconforming rough contacts in a vacuum. The thermal model was constructed based on the premise that the mean separation between the contacting surfaces in an infinitesimal surface element can be assumed constant. Therefore, the conforming rough model of Cooper et al.[13] could be implemented to calculate the surface element thermal resistance. The surface element thermal resistances were integrated over the macrocontact area to calculate the effective microthermal resistance of the contact. The macrocontact resistance was calculated using the flux tube solution.

The effects of the major contact parameters, that is, roughness, load, and radius of curvature, on TCR were investigated. It was shown that there is a value of surface roughness that minimizes TCR. Additionally, at large loads the effect of roughness on the TCR becomes negligible.

Through the use of the general pressure distribution introduced by Bahrami et al.[4] and the Yovanovich[15] correlation for thermal conductance of conforming rough contacts, simple correlations for determining TCR were derived that cover the entire range of TCR from conforming rough to smooth spherical contacts. The input parameters to utilize the proposed correlations are load F, effective elasticity modulus E', Vickers microhardness correlation coefficients c_1 and c_2, effective surface roughness σ and surface slope m, effective surface out-of-flatness δ or radius of curvature ρ, radius of the contacting surfaces b_L, and harmonic mean of the thermal conductivities k_s.

By the introduction of an approximate model for the microthermal resistance, it was shown that the microthermal resistance R_s is independent of the surface curvature and the profile of the contact pressure. Additionally, the micro- and the macrothermal resistances are functions of the micro- and macroscale contact parameters, respectively. The applied load appears directly in both resistances; the surface roughness influences the macrothermal resistance implicitly through the macrocontact radius.

The present model was compared with more than 600 experimental data points and showed good agreement over the entire range of TCR. The rms difference between the model and the data was estimated to be approximately 13.6%. The list of materials in the comparison formed a complete set of the metals used in applications where TCR is of concern. It was also shown that the present model is applicable to dissimilar metals.

A criterion for specifying the conforming rough contact was developed. A contact is conforming where the equivalent surface out-of-flatness is approximately between 3 and 30 times the equivalent surface roughness for very rough to very smooth surfaces, respectively.

References

[1]Clausing, A. M., and Chao, B. T., "Thermal Contact Resistance in a Vacuum Environment," TR ME-TN-242-1, Univ. of Illinois, Urbana, IL, Aug. 1963.

[2]Yovanovich, M. M., "Overall Constriction Resistance Between Contacting Rough, Wavy Surfaces," *International Journal of Heat and Mass Transfer*, Vol. 12, 1969, pp. 1517–1520.

[3]Mikic, B. B., and Rohsenow, W. M., "Thermal Contact Conductance," Dept. of Mechanical Engineering, TR NASA CN NGR 22-009-065, Massachusetts Inst. of Technology, Cambridge, MA, Sept. 1966.

[4]Bahrami, M., Culham, J. R., Yovanovich, M. M., and Schneider, G. E., "Thermal Contact Resistance of Non-Conforming Rough Surfaces, Part 1: Mechanical Model," *Journal of Thermophysics and Heat Transfer*, Vol. 18, No. 2, 2004, pp. 209–217; also AIAA Paper 2003-4197, June 2003.

[5]Bahrami, M., Culham, J. R., Yovanovich, M. M., and Schneider, G. E., "Review Of Thermal Joint Resistance Models For Non-Conforming Rough Surfaces In A Vacuum," American Society of Mechanical Engineers, Paper HT2003-47051, July 2003.

[6]Carslaw, H. S., and Jaeger, J. C., *Conduction of Heat in Solids*, 2nd ed., Oxford Univ. Press, London, 1959.

[7]Nishino, K., Yamashita, S., and Torii, K., "Thermal Contact Conductance Under Low Applied Load in a Vacuum Environment," *Experimental Thermal and Fluid Science*, Vol. 10, 1995, pp. 258–271.

[8]Lambert, M. A., and Fletcher, L. S., "Thermal Contact Conductance of Spherical Rough Metals," *Transactions of ASME: Journal of Heat Transfer*, Vol. 119, No. 4, Nov. 1997, pp. 684–690.

[9]Lambert, M. A., "Thermal Contact Conductance of Spherical Rough Metals," Ph.D. Dissertation, Dept. of Mechanical Engineering, Texas A&M Univ., College Station, TX, 1995.

[10]Clausing, A. M., and Chao, B. T., "Thermal Contact Resistance in a Vacuum Environment," *Journal of Heat Transfer*, Vol. 87, 1965, pp. 243–251; also American Society of Mechanical Engineers, Paper 64-HT-16, May 1964.

[11]Hertz, H., "On the Contact of Elastic Bodies," *Journal fur die reine und angewandie Mathematic*, Vol. 92, 1881, pp. 156–171 (in German).

[12]Yovanovich, M. M., Burde, S. S., and Thompson, C. C., "Thermal Constriction Resistance of Arbitrary Planar Contacts with Constant Flux," Progress in Astronautics and Aeronautics: Thermophysics of Spacecraft and Outer Planet Entry Probes, Vol. 56, P126, 1976; also AIAA Paper 76-440.

[13]Cooper, M. G., Mikic, B. B., and Yovanovich, M. M., "Thermal Contact Conductance," *International Journal of Heat and Mass Transfer*, Vol. 12, 1969, pp. 279–300.

[14]Yovanovich, M. M., "Recent Developments In Thermal Contact, Gap and Joint Conductance Theories and Experiment," *Eighth International Heat Transfer Conference*, American Society of Mechanical Engineers, Fairfield, NJ, 1986, pp. 35–45.

[15]Yovanovich, M. M., "Thermal Contact Correlations," *Spacecraft Radiative Transfer and Temperature Control*, edited by T. E. Horton, Progress in Aeronautics and Aerodynamics, Vol. 83, AIAA, New York, 1982, pp. 83–95; also AIAA Paper 81-1164.

[16]Hegazy, A. A., "Thermal Joint Conductance of Conforming Rough Surfaces: Effect of Surface Micro-Hardness Variation," Ph.D. Dissertation, Dept. of Mechanical Engineering, Univ. of Waterloo, Waterloo, ON, Canada, 1985.

[17]Song, S., and Yovanovich, M. M., "Relative Contact Pressure: Dependence on Surface Roughness and Vickers Microhardness," *Journal of Thermophysics and Heat Transfer*, Vol. 2, No. 1, 1988, pp. 43–47.

[18]Sridhar, M. R., and Yovanovich, M., "Empirical Methods to Predict Vickers Microhardness," *WEAR*, Vol. 193, 1996, pp. 91–98.

[19]Burde, S. S., "Thermal Contact Resistance Between Smooth Spheres and Rough Flats," Ph.D. Dissertation, Dept. of Mechanical Engineering, Univ. of Waterloo, Waterloo, ON, Canada, 1977.

[20]Fisher, N. F., "Thermal Constriction Resistance of Sphere/Layered Flat Contacts: Theory and Experiment," M.S. Thesis, Dept. of Mechanical Engineering, Univ. of Waterloo, Waterloo, ON, Canada, 1987.

[21]Kitscha, W., "Thermal Resistance of the Sphere–Flat Contact," M.S. Thesis, Dept. of Mechanical Engineering, Univ. of Waterloo, Waterloo, ON, Canada, 1982.

[22]Milanez, F. H., Yovanovich, M. M., and Mantelli, M. B. H., "Thermal Contact Conductance at Low Contact Pressures," AIAA Paper 2003-3489, June 2003.

[23]Antonetti, V. W., "On the Use of Metallic Coatings to Enhance Thermal Conductance," Ph.D. Dissertation, Dept. of Mechanical Engineering, Univ. of Waterloo, Waterloo, ON, Canada, 1983.

[24]McMillan, R., and Mikic, B. B., "Thermal Contact Resistance with Non-Uniform Interface Pressures," Dept. of Mechanical Engineering, TR NASA CN NGR 22-009-(477), Massachusetts, Inst. of Technology, Cambridge, MA, Nov. 1970.